GA–A26002

THE GENERAL ATOMICS FUSION THEORY PROGRAM REPORT FOR GRANT YEAR 2005-2007

by
PROJECT STAFF

FEBRUARY 2008

DISCLAIMER

GA–A26002

THE GENERAL ATOMICS FUSION THEORY PROGRAM REPORT FOR GRANT YEAR 2005-2007

by
PROJECT STAFF

Work supported by
the U.S. Department of Energy
under Grant No. DE-FG03-95ER54309

GENERAL ATOMICS PROJECT 03726
FEBRUARY 2008

Abstract

The objective of the fusion theory program at General Atomics (GA) is to significantly advance our scientific understanding of the physics of fusion plasmas and to support the DIII-D and other tokamak experiments as well as ITER research activities. The program plan is aimed at contributing significantly to the Fusion Energy Science, the Tokamak Concept Improvement, and ITER goals of the Office of Fusion Energy Sciences (OFES). Significant progress was made in each of the important areas of our research program during the last grant period GY05-07. This includes development of a new theoretical model for edge localized mode (ELM)-free quiescent high confinement mode, development of a new trapped gyro-Landau fluid (TGLF) transport model with comprehensive physics, advancement of two novel Alfvén wave current-drive mechanisms to explain the central counter current drive in DIII-D hybrid discharges, demonstration of full GYRO simulations of coupled ion temperature gradient/trapped electron mode-electron temperature gradient (ITG/TEM-ETG) turbulence with a number of striking conclusions, demonstration that the 3D magnetohydrodynamic (MHD) code NIMROD coupled with the atomic physics package KPRAD can qualitatively capture the sequence of events observed in C-Mod and DIII-D massive gas injection (MGI) disruption mitigation experiments, quantitative evaluation of the Porcelli sawtooth crash criteria through a complete giant sawtooth cycle, demonstration using the 3D MHD code NIMROD that the resonant magnetic perturbation (RMP) field can be screened out when edge rotation exceeds a critical value, demonstration of the turbulent momentum pinch effects necessary for very low toroidal rotation states observed in C-Mod and DIII-D in over 100 GYRO simulations, and development of a stopping model that explains the lack of direct penetration of broad supersonic gas jets during MGI experiments in current tokamak experiments.

1. Highlights of Theory Work in GY05-07

During the past 3 years, significant progress was made in each of the important areas of our research program:

- Development of a new theoretical model for edge localized mode (ELM)-free quiescent high confinement mode (QH-mode) discharges in which the edge harmonic oscillation (EHO) is a saturated kink-peeling mode that drives transport allowing a near steady-state plasma edge.

- Development of a new, trapped gyro-Landau fluid (TGLF) transport model with comprehensive physics including general magnetic geometry and finite beta with an extended range of validity compared to its predecessor GLF23.

- Advancement of two novel Alfvén wave current-drive mechanisms due to rotating magnetic islands to explain the central counter current drive in DIII-D hybrid discharges.

- Demonstration using coupled ion-temperature gradient (ITG), trapped-electron mode (TEM), and electron-temperature gradient (ETG) turbulence simulations with GYRO that ITG/TEM and ETG transport processes are not strongly coupled, but coupled simulations are necessary for accurate turbulence spectrum, and spectral isotropy eases high-k diagnostic measurements.

- Demonstration that the 3D magnetohydrodynamic (MHD) code NIMROD coupled with the atomic physics package KPRAD can qualitatively capture the sequence of events observed in C-Mod and DIII-D massive gas injection (MGI) disruption mitigation experiments.

- Quantitative evaluation of the Porcelli sawtooth crash criteria through a complete giant sawtooth cycle for a DIII-D neutral beam injection (NBI) and fast wave (FW) heated discharge that shows consistency with the observed crash when the ideal and fast-ion contributions to the crash criteria are accurately computed using GATO and ORBIT-RF/TORIC.

- Development of a formulation to evaluate the kinetic effect of particle drift and bounce motions on MHD modes in terms of the induced anisotropic pressure for slowly rotating tokamak plasmas.

- Demonstration using the 3D MHD code NIMROD that the resonant magnetic perturbation (RMP) field in a DIII-D RMP discharge can be screened out almost entirely when the edge rotation is above ~30 km/s.

- Demonstration of the turbulent momentum pinch effects necessary for very low toroidal rotation states observed in C-Mod and DIII-D spontaneous rotation discharges in over 100 GYRO simulations.

- Development of a stopping model that explains the lack of direct penetration of broad supersonic gas jets during MGI experiments in current tokamak experiments with the stopping force provided by the plasma ablation pressure.

- Demonstration that a moderate ratio of edge to internal transport barrier height in double-barrier plasmas is beneficial to ideal MHD stability and the stability is limited by global low-n modes.

- Demonstration using resistive MHD stability calculations that show reduction of axial q toward 1 plays a key role in the onset of 2/1 tearing modes in DIII-D hybrid discharges and that full matrix calculations including tearing and interchange coupling are necessary to explain the experimental observations.

- Verification of the importance of phasing angle in the magnetic feedback stabilization of resistive wall modes (RWMs) as observed in DIII-D experiments from modeling with the MARS-F MHD code.

- Derivation of a formula based on neoclassical theory with large toroidal flow that qualitatively resolves the discrepancy between predictions from NCLASS and DIII-D measurements.

- A 64-bit parallel version of the global convergent Newton method solver GCNMP was developed that includes the basic tokamak transport equations with GLF23 as the primary energy transport vehicle.

- Demonstration that the changes in sawtooth behavior in a DIII-D fast-wave heated discharge can be qualitatively modeled with the Kadomtsev mixing model and an appropriately chosen triggering parameter using the ONETWO transport code.

As a consequence of these results, scientists from the Theory Group were selected to give a number of invited talks and colloquia as highlighted in the next section. Section 3 provides more detailed descriptions of the advances and achievements made in each of the major areas.

2. Significant Presentations in GY05-07

2.1. 2007 Presentations

49th APS DPP Meeting in Orlando, Florida, November 12-16, 2007:

- J.E. Kinsey gave an invited presentation "First Transport Code Simulations Using the TGLF Model."
- V.A. Izzo gave an invited presentation "MHD Simulations of Disruption Mitigation on DIII-D and Alcator C-Mod."

International Sherwood Fusion Theory Conference in Annapolis, Maryland, April 23-25, 2007:

- M. Choi gave an invited presentation "Interaction of Fast-Wave-Accelerated Beam Ions with Ideal Internal Kink Instability in the DIII-D Tokamak."

12th EU-US Transport Task Force Workshop in San Diego, California, April 17-20 2007:

- J. Candy gave a presentation "Progress on a Fully Gyrokinetic Transport Code."
- P.B. Snyder gave a presentation "Understanding the Power Dependence of the Pedestal."
- G.M. Staebler gave a presentation "TGLF Saturation Rule."

11th IAEA Technical Meeting on H-Mode Physics and Transport Barriers in Tsukuba, Japan, September 26-28 2007:

- P.B. Snyder gave a presentation "Physics Understanding of the Pedestal Power Dependence: Implications for a First Principle Pedestal Model."

7th Symposium on Current Trends in International Fusion Research — A Review in Washington, DC, March 5-9, 2007:

- V.A. Izzo gave an invited presentation "NIMROD Extended MHD Simulations for Disruption Mitigation Studies."

3rd IAEA Technical Meeting on the Theory of Plasma Instabilities in York, United Kingdom, March 26-28, 2007:

- J. Candy gave a presentation "Status of Gyrokinetic Transport Modeling for ITER."

SciDAC 2007 Conference in Boston, Massachusetts, June 25-28, 2007:

- J. Candy gave a presentation "Plasma Microturbulence Simulation of Instabilities at Highly Disparate Scales."

6th Workshop on Nonlinear Plasma Science in Suzhou-Hangzhou, China, September 21-26, 2007:

- M.S. Chu gave a presentation "Feedback Stabilization of Neoclassical Tearing Modes Using ECCD."

17th Topical Conference on Radio Frequency Power in Plasma in Clearwater, Florida May 7-9, 2007:

- M. Choi gave a presentation "Effect of Energetic Trapped Particles Produced by ICRF Wave Heating on Sawtooth Instability in the DIII-D Tokamak."

34th European Physical Society Conference on Plasma Physics in Warsaw, Poland, July 2-6, 2007:

- J. Candy gave a presentation "Progress on a Fully Gyrokinetic Transport Code."

2.2. 2006 Presentations

21st IAEA Fusion Energy Conference in Chengdu, China, October 16-21, 2006:

- J. Candy gave an oral presentation "Coupled ITG/TEM-ETG GyroKinetic Simulations."
- M.S. Chu gave an oral presentation "Mechanism for Maintaining the Quasi-Steady State Central Current Density Profile in Hybrid Discharges."
- P.B. Snyder gave an oral presentation "Stability and Dynamics of the Edge Pedestal in the Low Collisionality Regime: Physics Mechanism for Steady-State ELM-Free Operation."
- G.M. Staebler gave an oral presentation "A Comprehensive Theory-Based Transport Model."

48th APS DPP meeting in Philadelphia, Pennsylvania, October 30 through November 3, 2006:

- D.P. Brennan gave an invited presentation "Resistive Stability of 2/1 Modes Near 1/1 Resonance."
- G.M. Staebler gave an invited presentation "A Theory-Based Transport Model with Comprehensive Physics."

- R.E. Waltz gave an invited presentation "Coupled ITG/TEM-ETG GyroKinetic Simulations."

Combined 2006 APS and Sherwood meeting in Dallas, Texas April 22-25, 2006:

- J.E. Kinsey gave an invited presentation "Parametric Dependencies of Transport Using Gyrokinetic Simulations Including Kinetic Electrons."

TTF meeting in Myrtle Beach, South Carolina, April 4-7, 2006:

- J. Candy gave an oral presentation "The GYRO Code: Turbulence in Tokamak Plasmas."
- P.B. Snyder gave an oral presentation "Nonlinear Dynamics and Transport Mechanisms for ELMs: Physics of ELM-free QH and RMP Discharges."

ITER Simulation Workshop in Beijing, China, May 15-17, 2006:

- V.S. Chan gave an invited presentation "Monte-Carlo Simulation of ICRF Wave Interactions with Energetic Particles in Tokamak Plasmas."
- L.L. Lao gave an invited presentation "Tokamak and ITER Equilibrium Reconstruction."
- R.E. Waltz gave an invited presentation "Continuum GyroKinetic Simulations and GyroFluid Models."

SciDAC 2006 Conference in Denver, Colorado, June 25-29, 2006:

- D.P. Brennan gave an invited presentation "Computing Nonlinear Magnetohydrodynamic Instabilities in Fusion Plasmas."

Workshop on Theory of Fusion Plasmas in Varenna, Italy, August 28 through September 1, 2006:

- A.D. Turnbull gave an invited presentation "Monte-Carlo Simulation of High Harmonic Fast Wave Heating of Neutral Beam Ions and Effects on MHD Stability: Validation with Experiments."

11th EU-US Transport Task Force Workshop in Marseille, France, September 4-7 2006:

- J. Candy gave an oral presentation "ETG Turbulence Coupled to ITG/TEM Turbulence."
- J.E. Kinsey gave an oral presentation "Database of GyroKinetic Transport Simulations and Comparison to a New Comprehensive Theory-Based Transport Model."

2.3. 2005 Presentations

2005 International Sherwood Fusion Theory Conference in Stateline, Nevada, April 11-13, 2005:

- D.P. Brennan gave an oral presentation "Nonlinear Evolution of Edge Localized Modes."
- J. Candy gave an oral presentation "the General Atomics DROP Cluster."
- C. Estrada-Mila gave an oral presentation "Gyrokinetic Simulations of Ion and Impurity Transport."

32nd EPS Plasma Physics Conference in Tarragona, Spain, June 27 through July 1, 2005:

- P.B. Snyder gave an oral presentation "Nonlinear Dynamics and Energy Loss Mechanisms of ELMs."

16th Topical Conference on Radio Frequency Power in Plasmas in Park City, Utah, April 11-13, 2005:

- M. Choi gave an invited presentation "Monte-Carlo Orbit/Full-Wave Simulation of Fast Alfvén Wave Damping on Resonant Ions in Tokamaks."

9th Joint US-European TTF Workshop in Napa, California, April 6-9, 2005:

- J. Candy gave an oral presentation "History of GYRO Verification and Suggestions for Future Development Practices."
- P.B. Snyder gave an oral presentation "Dual Transport Mechanisms for ELMs."

UCLA-PAM Workshop on "Multi-scale Processes in Fusion Plasmas" in Los Angeles, California, January 10-14, 2005:

- R.E. Waltz gave an invited presentation "Gyrokinetic Simulations and Multi-scale Processes."

2005 Cray User Group (CUG) Meeting in Albuquerque, New Mexico, May 16-19, 2005:

- J. Candy gave an oral presentation "GYRO Performance on MPP Systems."

US-Japan JIFT Workshop on Integrated Modeling of Multi-scale Physics in Fusion Plasmas in Kyushu, Japan, September 13-15, 2005:

- V.S. Chan gave an oral presentation on "Simulation of ICRF Interactions with Fast Ions and Modification of MHD Stability."

3. Advances in Transport Research

3.1. GYRO Development and Applications

GYRO work over this grant period was focused on the simulation of short-wavelength ETG transport including kinetic ion physics. The highly challenging issue of nonlinear coupling of short-wavelength ETG turbulence to long-wavelength physics (i.e., ITG and TEM turbulence) was explored. This multi-scale coupling problem was the subject of much prior speculation. A significant DOE (INCITE) computer time award in 2006 allowed us to determine the nature of this coupling at reduced ion-to-electron mass ratio. It was found that electron density fluctuations in high-resolution kinetic ion simulations are highly isotropic without radially-elongated "streamers".

Streamers are found to exist only in unphysical small box ($8\rho_i \times 8\rho_i$) ETG-ki simulations where the ion gyroscale low wave numbers $0 < k_\theta \rho_i < 1$ are neglected, as shown in Fig. 1(a). No streamers are seen in the more physical larger box ($64\rho_i \times 64\rho_i$) simulations shown in Fig. 1(b) at the same spatial resolution and plasma conditions. Remarkably, the total ETG-ki electron thermal transport ($k_\theta \rho_i < 1$) is the same for both simulations (even if the spectrum of transport differs). This demonstrated that larger than expected ETG transport does not depend on the existence of streamers, which are broken up by the ion gyroscale eddies.

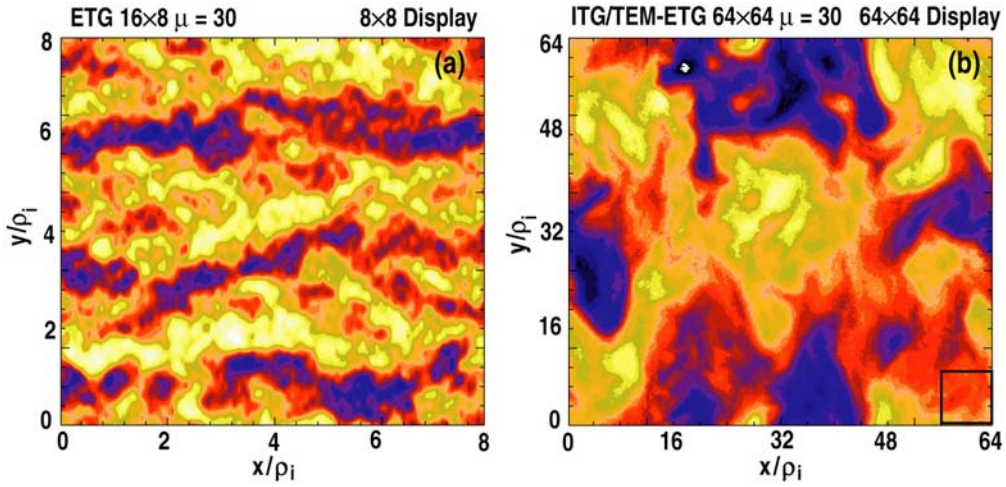

Fig. 1. Electron density contours for ETG simulations in a small box (a) compared to a more physical large box (b) showing that streamers in (a) are broken up by large ion gyroscale eddies in (b). Same resolution and GA-standard case parameters. The length y is along the flux surface perpendicular to the magnetic field and length x is across the flux surface.

During GY07, simulations exploring the effect of plasma shaping were focused on reversed triangularity (δ) and compared those results with the qualitative trends observed on TCV. GYRO results show that increasing δ is destabilizing while decreasing δ is stabilizing. This is illustrated in Fig. 2. These results are in qualitative agreement with recent TCV observations from a series of L-mode experiments. The simulations included kinetic electrons and were assumed to be electrostatic. As δ was varied, all other local quantities were held fixed (including κ) using the Miller equilibrium model. The effect of δ is found to be greatest for moderately elongated plasmas. The destabilizing effect on transport for positive δ in the plasma edge region can act to counter any improvement in MHD stability and both effects need consideration when studying the H-mode pedestal region.

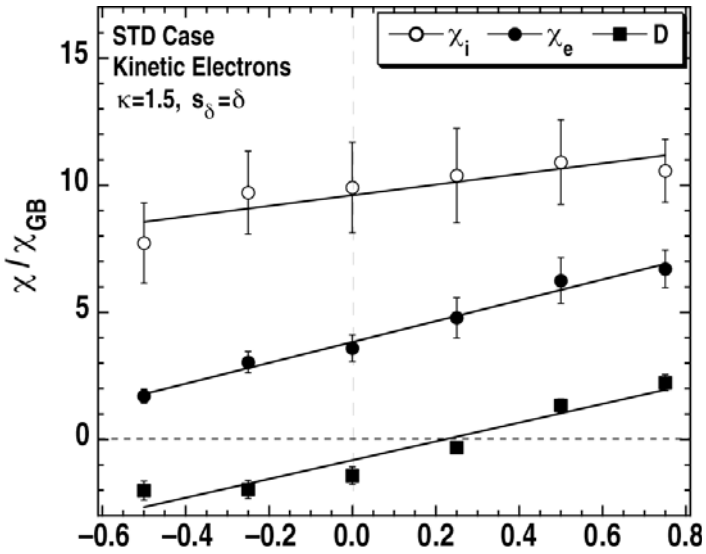

Fig. 2. Time-averaged ion diffusivities versus triangularity for an elongation of 1.5 from GYRO nonlinear simulations with kinetic electrons around the STD case.

Large coupled ITG/TEM-ETG GYRO simulations were carried out during GY07. These coupled simulations of ECH and Ohmic DIII-D discharges were the first to use actual experimental parameters, including an ion to electron mass ratio of 3600. Contrary to previous coupled collisionless simulations, the high collisionality, consistent with the actual physical parameters, induced significant anisotropy in the high-k turbulence spectrum. High-k diagnostics measure along the k_x (radial) axis whereas the ETG transport is carried on the k_y (near poloidal) axis. In the Ohmic case, the very high collisionality damped out the TEM transport making the 42% electron energy transport from ETG ($k_y \rho_* > 1$) unusually high. Even with reduced box size and resolution of these simulations, each run took 36 hours on 640 processors of the CRAY XT-4. Larger box-size higher-resolution runs are needed to fully confirm these results.

Additionally, local GYRO gyrokinetic simulations of a DIII-D L-mode discharge are able to simultaneously reproduce experimentally measured ion and electron heat diffusivities as well as the root-mean-square (RMS) density fluctuation levels measured by beam emission spectroscopy (BES) at mid-radius ($\rho = 0.5$). Synthetic BES signals, which account for the finite wave number sensitivity of the volume-sampling measurement, are generated from GYRO to perform quantitative comparisons with the experimental signals. In contrast, local simulations of the outer core ($\rho = 0.75$) are found to under predict the ion and electron heat fluxes by a factor of 4. The synthetic RMS density fluctuations at this location are less than half of the level measured by BES. Additional comparisons of frequency spectra and correlation lengths, as well as to T_e fluctuations obtained by the new correlation electron cyclotron emission (CECE) diagnostic, are underway.

Finally, the toroidal angular momentum diagnostic in GYRO was reformulated starting with moments of the 6D kinetic equation in Cartesian velocity space as outlined in Staebler's 2004 work. The spontaneous (or intrinsic) toroidal rotation found in C-Mod and DIII-D when there is no obvious external source of toroidal angular momentum are very low toroidal rotation states which require momentum "pinch" effects. For these states, the ratio of effective momentum diffusivity to effective ion energy diffusivity is zero rather than of order unity as normal driven states with large toroidal rotation. There are two sources of momentum pinch effects: The Dominguez-Staebler 1993 $E \times B$ shear effect (in slab geometry) and the Peeter-Angioni-Strinzi 2006 finite parallel velocity curvature drift effect (in toroidal geometry). From over 100 GYRO simulations we can now clearly demonstrate these pinch effects at low rotation. Correctly modeling the spontaneous toroidal rotation will require these pinch effects to be built into the new TGLF transport model.

3.2. TGLF Transport Model Development

Considerable effort has been placed over this grant period on the development of the TGLF to replace GLF23. The 4-moment per species (and adiabatic ion ETG) model was replaced with a 15-moment gyrofluid closure spanning continuously from ITG/TEM to ETG wave numbers. The parameterized trial wave function of GL23 was replaced with an expansion in 4-Hermite polynomials allowing treatment of real shaped geometry. This makes for a larger 120×120 TGLF dispersion matrix compared to the 8×8 GLF23 matrix. Linear TGLF growth rates are still obtained hundreds of times faster than the GKS code to 11% accuracy (GKS-GYRO agreement is also 11%). Previous GLF23 growth rate accuracy varied from 21% in core, 32% for NCS, to 54% in the pedestal. TGLF linear stability profiles and spectra are now available and are being used for DIII-D experimental planning and analysis. The TGLF fluctuation intensity saturation rule was

fit to a database of 86 s-α GYRO flux tube simulations in the GYRO database. The result is a dramatic improvement over GLF23.

During GY07, methods to speed up the Newton implicit time-step with TGLF were identified. The TGLF eigenmodes are computed in two stages. The first stage finds the Gaussian width that gives the maximum growth rate with one Hermite basis function. The second stage uses this width and refines the solution with four Hermite basis functions. Each stage takes about the same amount of CPU time. A subroutine that pre-computes the optimum width and stores it along with the eikonal functions evaluated at the Hermite nodes was written.

The saturation rule for TGLF was finalized for both Miller and shifted circle geometries using a large GYRO transport database of over 150 simulations. The XPTOR transport code was also ported to the Drop Linux cluster. TGLF was implemented in XPTOR and tested. A version of TGLF using four unstable modes gave a somewhat better fit to GYRO TEM simulations than using two modes. For all other GYRO simulations, the two- and four-mode versions of TGLF fit equally well. However, in transport simuations using TGLF in XPTOR it was found that using two unstable modes yielded a better fit to experimental data resulting in the decision to use only two modes in the finalized version of the TGLF model for the 2007 APS meeting. Comparing the predicted temperatures from TGLF against a large L-mode and H-mode database of 96 discharge we find that TGLF yields somewhat lower rms errors than GLF23 using the same methodology in XPTOR. The rms error in the incremental stored energy is 32% for TGLF and 37% for GLF23. This is shown in Fig. 3.

The average rms errors in the ion and electron temperature profiles are 24% and 19% for TGLF and 30% and 19% for GLF23. Over the entire database, the agreement for the T_e profiles is the same for the two models, but TGLF demonstrates lower errors than GLF23 for the T_i profiles. However, for DIII-D H-modes we do find lower T_e errors for TGLF (9.5%) than for GLF23 (12%). Overall, the best agreement for TGLF is obtained for DIII-D H-modes and the worst agreement is found for JET and TFTR, particularly for older shots. We also tested a shifted circle version of TGLF and find that it does not agree with experimental data as well as the Miller geometry version.

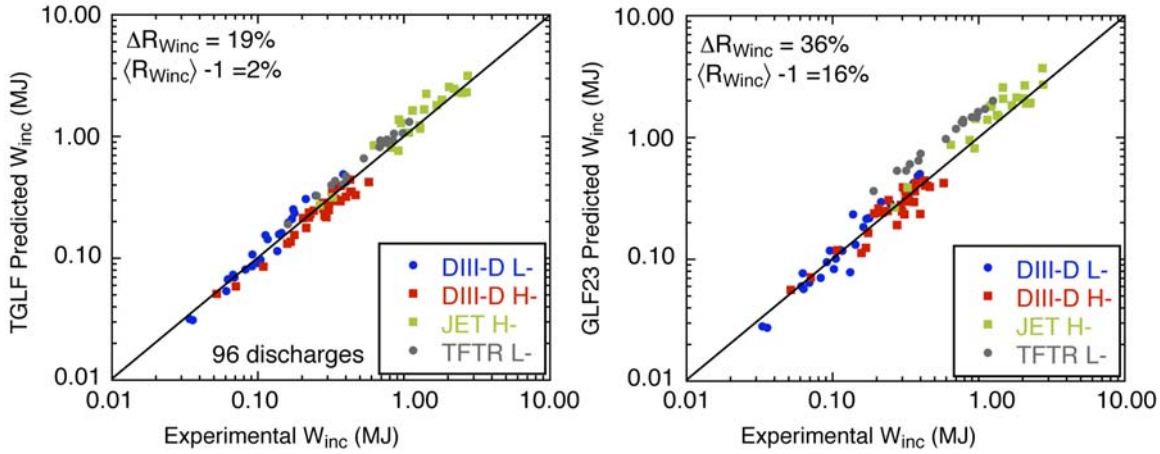

Fig. 3. TGLF and GLF23 predicted versus experimental incremental stored energy for 96 L-mode and H-mode discharges from DIII-D, JET, and TFTR.

3.3. Transport Code and Module Development

A 64-bit parallel version of the Globally Convergent Newton Method (GCNMP) solver was developed. The solver includes the basic tokamak transport equations as originally developed for the ONETWO code with GLF23 as the primary energy transport vehicle. The modular nature of GCNMP allows it to interact with all transport related physics codes (e.g. neutral beam, rf heating and current drive, MHD, etc.) In addition, GCNMP can utilize adaptive grids (variable size and spacing) and a variable number of equations by simply creating state files that include the necessary information.

During GY07, a new coupling interface for GCNMP was also developed using PYTHON procedure calls that allow a general client to request a service from the GCNMP server. The server can be on a remote host or reside on the same host as the client. It is expected that the client will run on a suitable single processor machine while the server will take full advantage of the parallel hardware it is running on. Tests using Linux workstations show that such an arrangement is satisfactory. During actual use, the client will make repeated calls to the server to advance the transport equations. All intervening input/output is through a state file. A development path was also initiated that will allow single source files to serve as common components for different projects.

A new version of the ONETWO transport code was developed that features full integration of the NUBEAM NTCC module, as well as the ability to run simpler and faster NFREYA-derived beam calculations for between-shot analysis in DIII-D. The NTCC Multi-mode confinement module MM95 was also added to ONETWO. A 64-bit version was also created that includes an interface to the new parallel GCNMP. The 64-bit version reduces the CPU time by about ~30%. As a first step to start implementation

of the TGLF transport model into ONETWO, work to reformulate the GCNMP solver using flow-based form of the transport equations was initiated.

3.4. Transport Theory Development

Turbulence not only causes energy transport (the dominant effect) but can also provide some small ohmic heating from fluctuations in the parallel and perpendicular-drift currents. Some months ago an important sign error was discovered in the Hinton-Waltz gyrokinetic heating formulation paper, which made the drift component cooling rather than the originally estimated heating. Subsequently we showed analytically that the local average of the combined heating and cooling was actually a small energy exchange between electrons and ions with no net plasma heating. GYRO flux tube simulations of the GA-standard case have now verified the analysis. A "full physics" global GYRO simulation of a DIII-D L-mode shows that the heating and cooling power flow is typically about 10% of the energy transport flows. It has always been somewhat unclear how to formulate this exchange using quasi-linear recipes needed to build models like GLF23 and TGLF. We now have shown that the quasi-linear recipe used in TGLF (carefully applied) gives a perfect exchange and a good match to the GYRO simulations. The energy exchange is being added to TGLF.

During the last grant period, we have also revisited a ~30-year old calculation of neoclassical angular momentum flux [Rosenbluth 1971]. We were able to make a clearer formulation of the problem, using the technique of the adjoint equation, in conjunction with distribution functions obtained by the method of matched asymptotic expansions that we applied earlier to neoclassical theory. By comparing the fluid and the drift-kinetic approaches in the Pfirsch-Schlüter regime, we have resolved a discrepancy between a recent [Catto 2005] and an earlier work [Hazeltine 1974]. It was discovered in the process that the poloidal electric field plays an important role. Re-examination of the calculation in the banana regime suggests that the neglect of the poloidal electric field is unjustified.

4. Advances in MHD Stability Research

4.1. Edge Stability and ELM Onset

During the last grant period, significant advances were made in the edge stability and ELM area. These include development of a new theoretical model for ELM-free QH-mode discharges, which postulates that QH mode exists in the low collisionality regime in which the edge bootstrap current is large, and the limiting instability is a relatively low-n kink/peeling mode rather than the usual intermediate-n peeling-ballooning modes responsible for ELMs. Strong flow shear in the QH mode edge stabilized high-n ballooning modes, but actually destabilizes low-n kink/peeling modes. These low-n kink/peeling modes, driven unstable both by current and rotation, are postulated to be responsible for the EHO observed during QH mode. The modes are able to saturate, rather than grow explosively like ELMs, due to their ability to dissipate their drive at relatively low mode amplitudes, via transport and coupling to the conducting wall. Transport driven by the saturated mode allows near steady state operation in QH mode.

Extensive QH mode stability calculations support this model, including accurate predictions of the required density for QH mode operation in various shapes, and edge stability effects in QH mode with both counter- and mixed co- and counter-neutral beam injection. We find that QH mode discharges consistently lie near the peeling (current-driven mode) stability boundary on edge stability diagrams.

In another study, a large set of 2006 DIII-D RMP discharges in which ELMs are suppressed with an imposed RMP was also studied with ELITE. It is generally found that the RMP allows the discharge to maintain steady state pressure and current profiles below the peeling-ballooning stability boundary, allowing ELM-free operation.

Since the pedestal stability constraint imposes a strong correlation between pedestal height and width ($\beta_{Nped} \sim \Delta^{3/4}$), it can be difficult to discern the separate physics of the pedestal width itself. Previous studies of the effect of Shafranov Shift and pedestal width variation on peeling-ballooning stability were extended to evaluate the feasibility of pedestal width models in which the pedestal width varies with global or local pedestal quantities. Here, the peeling-ballooning constraint is explicitly calculated so that it can be accounted for. The remaining physics of the pedestal width can then be evaluated. It is found that models in which the width varies with global quantities such as global beta cannot explain the disparate observed behavior at low and high triangularity. Models in

which the pedestal width varies with local pedestal quantities appear to be consistent with observations.

Many improvements to ELITE and benchmarking calculations with other codes were also made. In an extensive set of code benchmarking exercises, excellent agreement was found among ELITE, GATO and DCON, to better than 5% in the onset threshold for edge-localized modes when the equilibria are sufficiently well resolved. These results are summarized in Fig. 4. MHD stability codes are widely used to study tokamak stability, and recently have been used to study onset conditions for ELMs and the resulting constraints on the height of the edge barrier (or pedestal). The benchmarking calculations considered both the growth rates of instabilities, as well as the onset thresholds for edge-localized modes. For under-resolved equilibria, the results naturally vary more due to differences between codes in the mapping onto high-resolution grids. The resolution commonly used in experimental studies ($n_R \times n_Z = 129 \times 129$ grid points from EFIT) is generally sufficient, allowing a difference between stability results that is substantially smaller than the experimental uncertainty. However, significant improvement in agreement between the codes is obtained by using higher resolution (257×257 or 513×513) equilibria.

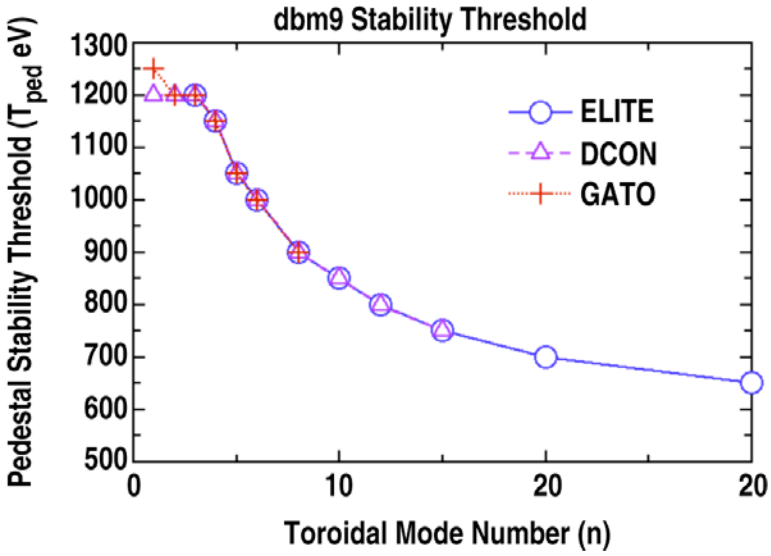

Fig. 4. In a D-shaped equilibrium with an H-mode pedestal, the pedestal temperature is increased at constant pedestal density until the threshold for MHD instability is found. A comparison of three MHD stability codes finds excellent agreement in the instability threshold as a function of toroidal mode number.

By extending the expansion of rotation terms to higher order, we have also found good quantitative agreement between the ELITE code and the MARS and CASTOR codes. The effect of sheared toroidal flows on growth rate, mode frequency and mode

structure has been confirmed with all three codes. The physics of flow shear effects, stabilizing high-n modes while having a weak or even de-stabilizing effect on lower n modes was confirmed.

4.2. Nonlinear ELM Study

Nonlinear ELM physics were studied using an enhanced version of the 3D reduced-Braginskii BOUT code. Several simulations of linearly unstable equilibria were undertaken, revealing the expected ballooning-like mode structure and growth rates at early times (and onset near the expected peeling-ballooning stability boundary), followed by bursts of one or many fast radially propagating filaments, similar to those observed during ELM crashes. An example of a case where many filaments in the linear case evolve into a dominant filament in the nonlinear phase is shown in Fig. 5(a). The simulations show some similarity to nonlinear ballooning theory, and suggest a two-prong model involving filament transport and partial barrier collapse as a mechanism for the full ELM losses.

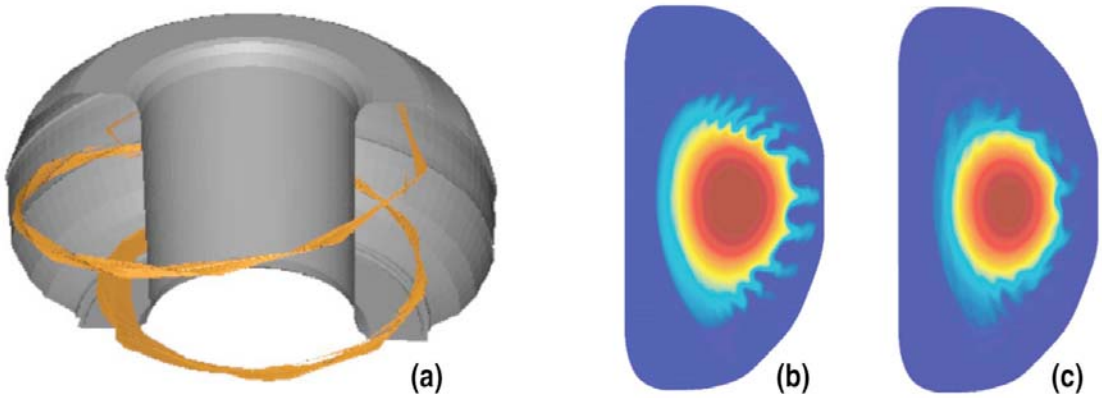

Fig. 5. (a) 3D BOUT simulation of the dynamic evolution of an ELM. In this case the multi-filamentary structure coalesces into a dominant filament as it propagates radially from the edge barrier region toward the outer wall of the DIII-D vessel. (b) ELM simulations using NIMROD show strong mode growth and deep mode penetration in the no-flow case. (c) Addition of toroidal flow localizes the mode radially and reduces heat flux to the outer wall.

The resistive MHD code NIMROD was also employed to study nonlinear ELM physics using several series of model experimental equilibria prepared with discharges from the DIII-D ELM experiments. The equilibria being used as initial conditions were distributed to CEMM for collaborating scientists to analyze and compare with our NIMROD results. All such results contribute to the DOE Theory Milestone for 2006. Studies using DIII-D discharges show that linearly unstable modes are in the range $5 < n < 25$ with the linear growth rates peaking at $n \sim 12$-15. Other modes are driven nonlinearly, some by two-wave interactions and some by three-wave interactions. The

time evolution of the kinetic energy in toroidal modes 1-43 shows that the nonlinear mode structure is toroidally resolved with finger like structures near the plasma edge. Increasingly fine structures appear as the calculation progresses. This is shown in Fig. 5(b,c). The penetration depth of the nonlinear mode into the plasma from the edge is in reasonable agreement with experiment. Toroidal flow shears the structure of the nonlinear mode, reducing the amplitude of fluctuations poloidally, and limits the extension of the filaments into the vacuum region, while having a smaller effect on the inward penetration.

During GY07, as an extension of previous RMP simulations with NIMROD, a scan over rotation profiles was also performed to examine the effects of rotation screening on the RMP fields and their associated transport. With high core rotation (~100 km/s) but low edge rotation (~1 km/s at the separatrix) some screening is observed at intermediate radii, but the enhanced particle transport is comparable to the no rotation case. At higher edge rotation (~30 km/s), the RMP fields are screened out almost entirely, and the enhanced transport is eliminated. A comparison of the screening results with analytic theory was done, with reasonable success in predicting the stochastic/good-flux-surface boundary based on theory for a cylindrical plasma.

4.3. Sawtooth Stability Modeling

Detailed sawtooth equilibrium and stability studies were carried out. Equilibrium reconstructions of a DIII-D FW discharge with motional Stark effect (MSE) and kinetic data using EFIT show that axial q_0 variations are much larger during the giant sawtooth phase than during the regular phase. q_0 varies between 0.96 and 1.01 during the regular phase with neutral-beam heating only, but between 0.85 and1.01 during the giant sawtooth phase with NBI plus FW. The axial q_0 variations correlate well with the application and change of FW power and central electron temperature from electron cyclotron emission (ECE).

Evaluation of the Porcelli sawtooth crash criteria through a complete giant sawtooth cycle was also carried out and shows consistency with the observed crash. While the Porcelli model using simplified expressions for the key contributions has been found to predict average sawtooth periods reasonably well in many cases, it is not completely adequate for quantitatively reproducing the actual crash time for a specific sawtooth in an experiment. The new calculations used the GATO code for the ideal contribution to the crash criteria for a series of six successive time slices during the sawtooth cycle, and the ORBIT-RF and TORIC codes to accurately calculate the non-Maxwellian fast-ion pressure and its kinetic contribution. Within the estimated uncertainties in the equilibrium reconstruction and fast ion distribution modeling, the calculations predicted the trigger

criterion becomes marginally satisfied right before the observed sawtooth crash. The results are summarized in Fig. 6.

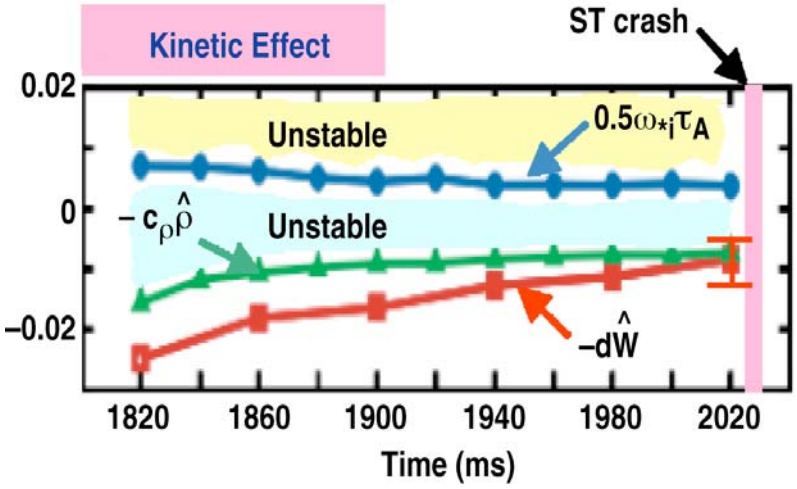

Fig. 6. Porcelli sawtooth crash criteria during the first giant sawtooth cycle from DIII-D discharge #96043. The sawtooth crash occurs at 2039 ms.

4.4. Resistive Wall Modes

Modeling of feedback stabilization with the MARS-F stability code yields an improved understanding of RWM active stabilization experiments using the internal I-coils in DIII-D. The optimum phasing angle of the upper and the lower I-coils with respect to the sensor signal was obtained and agrees with the experimentally measured angle. Moderate deviations from this phasing angle lead to a reduced feedback effectiveness. Large deviation of more than 90 degrees leads to a failure of the feedback, as expected from general theoretical expectations. This also correlates with the observation of disruptions in the experiments

During GY07, in collaboration with Professor Y.Q. Liu of Chalmers University, the kinetic effect of particle drift and bounce motions on MHD modes was formulated in terms of the induced anisotropic pressure due to the MHD motion for tokamak plasmas with toroidal flows. This formulation is thus suitable for treating slowly growing MHD modes where such effects are non-negligible, such as the internal kink or the resistive wall modes.

4.5. NIMROD/KPRAD Disruption Mitigation Simulations

During GY07, extensive simulations of Alcator C-Mod and DIII-D MGI disruption mitigation experiments using the NIMROD/KPRAD combined MHD/atomic physics code was carried out. NIMROD successfully captures the qualitative sequence of events

observed in MGI experiments with MHD playing an important role. Alcator C-Mod simulations was performed with both neon and helium gas jet injection. The time between the initial edge cooling and the core temperature collapse is found to be strongly dependent on the perpendicular thermal transport coefficient. However, with the coefficient set close to experimentally measure values, neon simulations predict very well the observed thermal quench onset time. Temperature profile evolution also matches experimental results quite well, but the edge density is much larger in the simulations than the experiments, which could be due to differences in transport or ionization fraction. Simulations with a pure helium gas jet considerably over predict the thermal quench onset time. However, C-Mod plasmas contain ~1% boron, which is a considerably better radiator than helium below 10 eV, show that even at that small fraction it could contribute as much to the total radiated power as the dense helium gas jet. Boron radiation was added to the helium jet simulations with the effect of increasing total radiated power during the initial jet penetration, and reducing the quench onset time. The addition of boron to the neon simulations also reduced the edge temperature and the neon ionization fraction, partially solving the primary discrepancy between the code and the experiments. A DIII-D helium jet simulation shows a faster rise time for total radiated power than the experiment, but comparable amplitude. Similar to the important role of boron in C-Mod, carbon radiation is a significant factor in DIII-D helium jet simulations and experiments.

4.6. Low n Ideal Stability Modeling

In an ideal stability study during the last grant period, it is found that a moderate ratio of edge to internal transport barrier height is beneficial to MHD stability and the stability is limited by global low-n modes (n is the toroidal mode number). Combining an internal transport barrier (ITB) with an H-mode edge transport barrier (ETB), i.e. producing a double transport barrier (DB) plasma, is a promising regime for advanced tokamak steady state operation with high beta. However, the large pressure gradient and the associated large bootstrap current at the transport barriers can drive MHD instabilities, which limit β. The stability study was carried out using model pressure and q profiles and plasma shape based on DIII-D experiments and the GATO ideal stability code. For moderate ITB width with weak ETB, the stability is limited by n = 1 global modes, whereas if the ETB is strong it is limited by moderate-n peeling-ballooning modes. Broadening ITB width can improve stability. For very broad ITB width DB plasmas, high-normalized β is obtained and the stability is limited by low-n (n > 1) modes.

In another study, the stability numerical problems for near-unity β D-shaped "current hole" case (having a region with essentially zero current on the inboard side of the magnetic axis) by P. Gourdain were fully resolved. The GATO results confirm this

equilibrium to be unstable to two internal modes, in contrast to the result obtained by Gourdain using DCON, which indicated internal mode stability. The equilibrium has $q_0 < 2$, rising to above 10 in midrange, and dropping back to just below 3 at the edge. The unstable modes are quite strongly localized inside the innermost $q = 2$ surface. The GATO result seems fairly robust and the mode growth rates converge to slightly more unstable as more flux surfaces are packed inside $q = 2$. Full convergence calculations are needed to obtain full confidence in the results.

4.7. Resistive Stability

In many DIII-D hybrid discharges, the high performance phase is terminated by the growth of a large 2/1 tearing mode. Analysis of DIII-D hybrid discharges just before onset of a 2/1 tearing mode finds that the tearing stability at $q = 2$ is highly sensitive to q_0 ($q_{\min}$) approaching unity, as a result of the ideal β_N limit rapidly decreasing toward the experimental β_N. The analysis is based on experimental equilibria with q_0 constrained within the uncertainty of the reconstruction between 0.98 and 1.05. Varying q_0 in this range results in little or no change in the equilibrium near q=2 or elsewhere. For $q_0 \geq 1.02$, the 2/1 tearing stability is only weakly dependent on β_N. However, when $q_0 \leq 1.01$, the 2/1 tearing mode (at $q = 2$) becomes strongly unstable as the equilibrium approaches the n=1 ideal limit. This suggests that the proximity to the $q = 1$ resonance is critical to the 2/1 tearing mode stability, and is responsible for the onset of the mode. The results suggest that the 2/1 onset may be prevented by a slight increase in q_0.

4.8. Non-Axisymmetric Plasma Response

During the last grant period, several key results were obtained in the theoretical formalism of the plasma response to external non-axisymmetric perturbations. For the linearized response, the conditions for completeness of the 2D eigenfunctions of the ideal MHD operator, as a basis for the plasma response, were obtained. Completeness can be lost following projection on the plasma boundary and then inversion back to the full plasma domain. In addition to the obvious case where internal modes exist, the conditions can be violated in certain well-defined situations that can be easily monitored and possibly avoided. In addition, the Nuhrenberg-Boozer application for determining the resonant displacement jumps and associated island sizes was generalized to any (including non-resonant) response feature. The generalization can then be applied to determine the specific externally applied perturbations needed to induce non-resonant perturbations, for independent control of MHD modes and plasma rotation. GATO continuum modifications will enable GATO to be utilized as a numerical tool to implement this formulation.

5. Advances in RF Heating and Fueling Research

5.1. Interactions of ICRF Wave With Ions

Resonant interaction between ions and ion cyclotron radio frequency (ICRF) wave at arbitrary cyclotron harmonics has been usually treated as a diffusive process in velocity space. This assumes de-correlation in the relative phase difference of the wave and ions between successive resonances. In a collisionless high temperature plasma, the change in trajectory of ions due to the change of energy through this interaction may produce a de-correlated phase. Since the de-correlation of phase difference depends strongly on the combination of applied amplitude of ICRF wave, the wave frequency, and the energy of ions, stochastic threshold amplitudes of the wave above which non-adiabatic interaction takes place may be very different in fundamental thermal minority ion heating (C-Mod) and high harmonic energetic beam ion heating (DIII-D) cases.

ORBIT-RF was applied to study the stochastic behavior of ion orbits and evaluate the stochastic threshold in the wave electric field amplitude using 2-D mapping in phase space on the C-Mod and DIII-D tokamaks. Numerical analysis of guiding center drift orbits using ORBIT-RF qualitatively agrees with the analytic stochasticity onset criterion in phase space obtained from the standard linear one-step mapping equation. For the analytic criterion, the orbit theoretically transitions from adiabatic to stochastic behavior when the stochastic onset parameter $S = 1$. S is related to the product of the perturbation amplitude and the change in phase from each rf kick. In addition to the wave amplitude, S depends on finite parallel wavelength, $k_{||}$, the finite Larmor radius, magnetic field inhomogeneity, pitch angle, and ion energy. All these parameters vary along the orbit in a realistic simulation and are expected to impact the threshold quantitatively. For fundamental harmonic heating, it is found that the threshold wave amplitude satisfying $S \geq 0.5$ is sufficient for onset of a stochastic trajectory, suggesting that the required threshold electric field might be smaller than the analytic prediction. A more rigorous criterion for the onset of stochasticity is being developed, which will be used to modify the quasi-linear model for wave interactions with energetic particles.

5.2. Alfvén Wave Counter Current Drive in Hybrid Discharges

The role of the 3/2 mode in maintaining the quasi-steady state central current density profile in DIII-D hybrid discharges was investigated. Two mechanisms that provide the negative central current drive were studied. All rely on the development of a large co-rotating 2/2 sideband excited by the rotating 3/2 island. In the first mechanism, the central

q_0 is assumed to develop to a value below the Alfvén resonance at the plasma center, yet above the value that initiates sawteeth. For the region within the Alfvén resonance, stationary kinetic Alfvén waves (KAW) are excited by the 2/2 sideband. The KAWs, due to their short perpendicular wavelengths, provide an efficient current drive counter to the plasma current within the resonant region. The amount of driven current increases quadratically with the size of the 2/2 sideband. In the second mechanism, the electric field sideband is excited by the 3/2 magnetic perturbations due to the magnetic curvature drift of the ions. This is a purely toroidal effect and contributes to the negative current drive over a larger range of q_0 values than the KAW mode conversion mechanism.

5.3. Massive Gas Injection

A stopping model that explains the universally observed lack of direct penetration of broad supersonic gas jets during MGI experiments in all current tokamak experiments was developed. The stopping force is the plasma plume (ablation) pressure surrounding the frontal cap of the neutral gas jet, which is communicated to the supersonic neutral interior region (untouched by incident plasma electrons) by means of a backward propagating shock wave. The plume pressure itself is regulated by the parallel expansion dynamics. We have specialized to argon jets with radiation cooling rates, and ionization potential energy changes derived from the CRETIN radiation code. From the point of view of the Maxwell stress tensor, the forward momentum lost by the jet is ultimately taken up by the toroidal magnetic field because the low β ablation plume digs a weak localized magnetic well.

Although the gas jet does not directly penetrate the plasma, experiments have shown that the some of the gas particles (ions) do end up inside the plasma. The efficacy of plasma densification can be quantified by introducing the "mixing efficiency." Mixing efficiencies for both the Mark IV and Medusa gas jets for various gas species: hydrogen, helium, neon, and argon were characterized using FLUENT. For Medusa jet typically helium has the highest mixing efficiency ~30%, while argon has the lowest ~0%. An analytical model for the diffusion of the impurity ions stopped at the plasma boundary was also developed to support these findings.

A 1D time-dependent fast quench code that models the evolution of the toroidal electric field and current density in the plasma was also developed to study the effect of various fueling sources on the current quench and runaway electron production. The model includes a thermal energy balance equation with radiation and heat transport. We have been concentrating on "volumetric fueling" by liquid jets or a train of pellets. Dilution cooling predominates during the propagation of deuterium jets/pellets. Because of this "mild cooling," large density increases are possible without appreciable modification of the current profile. After dilution cooling/injection is completed, the

plasma cools rapidly by bremsstrahlung radiation down to ~1 eV, whereupon recombination process take over and a balance state occurs between radiation loss and ohmic heating while the total plasma current decays. We have found that for ITER the current decays in ~50-100 ms, and no runaways are produced.

5.4. Pellet Ablation

A new physical effect was included in the 2D pellet ablation simulations: Cloud rotation about its axis caused by electrostatic charging of the ablation cloud interior by the penetrating plasma electrons. The negative cloud floating potential varies from axis to cloud boundary due to variation in the interception of the incident electron flux across field lines. As a result, there will be large radial electric field causing $E \times B$ rotation as previously suggested by Parks ten years ago. Rotation is important for two reasons. First, the rotation speed turns out to be comparable or even larger than the sound speed of the cloud ("supersonic rotation"). Preliminary simulations find that the rotation ablation cloud density profile becomes hollow as a result of the centrifugal force throwing interior matter against the outer "magnetic barrier". The reduced opacity in the pellet shadow region (near the axis) leads to less pellet shielding and consequently the ablation is increased. This is an exciting result because this increase may offset the factor of 2-3 decrease due to channel formation. This may leave the net ablation rate closer to the experimentally inferred value.

6. Advances in Innovative Confinement Concept and Integrated Modeling Research

6.1. 3D Equilibrium Reconstruction

In the last grant period, in collaboration with ORNL and Auburn University, substantial progress was made toward the development of the new 3D equilibrium reconstruction code, V3FIT. V3FIT is based on the VMEC 3D equilibrium code and the EFIT response function method. The EFIT response function method was generalized to 3D magnetic geometry and modules were developed to provide efficient evaluation of 3D magnetic responses to a diagnostic set. These response modules were applied to support design of magnetic diagnostics for NCSX and CTH. First V3FIT reconstructions were successfully carried out using two current-profile parameters to fit 12 model magnetic signals. Detailed benchmarking calculations against 2D EFIT equilibrium reconstruction results are ongoing. The V3FIT reconstruction algorithm is based on a pseudo-Newton least-square approach and is computationally intensive. To do a reconstruction, many VMEC equilibrium calculations are required to update the Jacobian and search for the minimum. To improve the search, various linearization schemes have also been formulated to approximate the signal gradients and to accelerate the search for the solution vector based on the efficient 2D EFIT optimization approach that interleaves the fitting and the equilibrium iterations.

6.2. Integrated Sawtooth Modeling

During GY07, an integrated analysis was carried out using the transport code ONETWO to model the changes in sawtooth behavior in DIII-D discharges after FW heating is applied due to interactions between FW and NBI fast ions with MHD stability. The evolution of q_0 within a sawtooth period is modeled using ONETWO with neoclassical resistivity and experimental density and temperature profiles. The results indicate that the predicted drops in q_0 within a sawtooth cycle follow closely the experimental values reconstructed from the EFIT code using MSE data. So far, most of the analyses are limited to a single sawtooth cycle. Initial analysis using the Kadomtsev sawtooth mixing model indicates that the sawtooth crash can be qualitatively reproduced with an appropriately chosen triggering parameter. The results are summarized in Fig. 7. The Porcelli sawtooth model is being implemented into ONETWO to more comprehensively simulate the sawtooth crash.

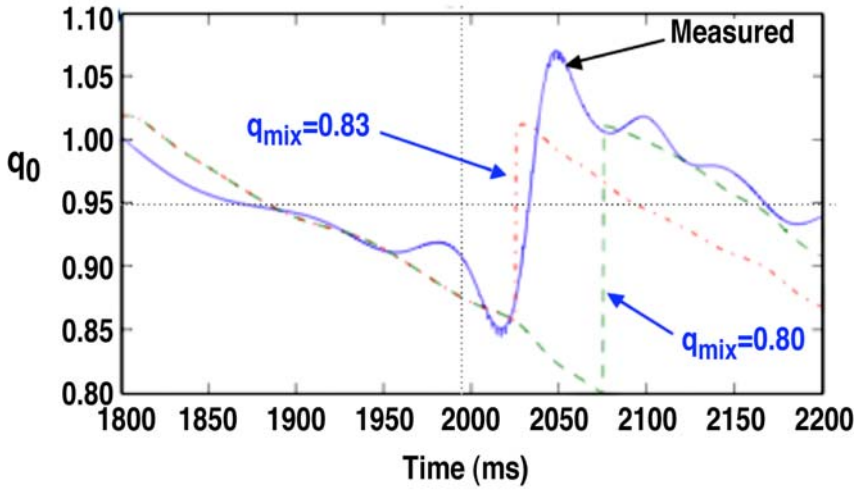

Fig. 7. Comparison of axial q_0 evolution during two giant-sawtooth cycles from ONETWO simulations using the Kadomtsev sawtooth mixing model with two different trigger parameters q_{mix} = 0.83 (blue curve) and 0.80 (green curve) for a DIII-D FW discharge against the experimental reconstructed values using EFIT with MSE and magnetic data.

7. Publications

7.1. Primary Theory Authors for 2007

D.P. Brennan, A.D. Turnbull, M.S. Chu, R.J. La Haye, L.L. Lao, T.H. Osborne, and S.A. Galkin, "Resistive Stability of 2/1 Modes Near 1/1 Resonance," Phys. Plasmas **14**, 056108 (2007).

J. Candy, R.E. Waltz, and M. Fahey, "The Efect of Ion-scale Dynamics on Electron-Temperature-gradient Turbulence," Plasma Phys. Control. Fusion **49**, 1209 (2007).

J. Candy, R.E. Waltz, M. Fahey, and C. Holland, "Plasma Microturbulence Simulation of Instabilities at Highly Disparate Scales," J. Phys. Conf. Series **78**, 012008 (2007).

M.S. Chance, A.D. Turnbull, P.B. Snyder, "Calculation of the Vacuum Green's Function Valid Even for High Toroidal Mode Number in Tokamaks" J. Comput. Phys. **221**, 330 (2007).

M. Choi, A.D. Turnbull, V.S. Chan, M.S. Chu, L.L. Lao, Y.M. Jeon, G. Li, Q. Ren, R.I. Pinsker, "Sawtooth Control Using Fast Wave-Accelerated Beam Ions in the DIII-D Tokamak," to appear in Phys. Plasmas.

M.S. Chu, D.P. Brennan, V.S. Chan, M. Choi, R.J. Jayakumar, L.L. Lao, R. Nazikian, P.A. Politzer, H.E. St. John, A.D. Turnbull, M.A. Van Zeeland, and R. White, "Maintaining the Quasi-steady Central Current Density Profile in Hybrid Discharges," Nucl. Fusion **47**, 434 (2007).

J.E. Kinsey, R.E. Waltz, J. Candy, "The Effect of Plasma Shaping on Turbulent Transport and E×B Shear Quenching in Nonlinear Gyrokinetic Simulations," Phys. Plasmas **14**, 102306 (2007).

G. Li, S.J. Wang, L.L. Lao, A.D. Turnbull, M.S. Chu, D.P. Brennan, R.J. Groebner, and L. Zhao, "Ideal MHD Stability of Double Transport Barrier Plasmas in DIII-D," to appear in Nucl. Fusion.

G.M. Staebler, J.E. Kinsey and R.E. Waltz, "A Theory Based Transport Model with Comprehensive Physics," Phys. Plasmas **14**, 055909 (2007).

P.B. Snyder, K.H. Burrell, H.R. Wilson, M.S. Chu, M.E. Fenstermacher, A.W. Leonard, T.H. Osborne, M. Umansky, W.P. West, and X.Q. Xu, "Stability and Dynamics of the Edge Pedestal in the Low Collisionality Regime," Nucl. Fusion **47**, 961 (2007).

R.E. Waltz, J. Candy, and M. Fahey, "Coupled Ion Temperature Gradient and Trapped Electron Mode to Electron Temperature Gradient Mode Gyrokinetic Simulations," Phys. Plasmas **14**, 056116 (2007).

S.K. Wong and V.S. Chan, "Fluid Theory of Angular Momentum Flux of Plasmas in an Axisymmetric Magnetic Field," Phys. Plasmas **14**, 112505 (2007).

S.K. Wong and V.S. Chan, "Kinetic Theory of Radial Angular Momentum Flux of Collisional Plasmas in an Axisymmetric Magnetic Field," to appear in Phys. Plasmas (2007).

7.2. Primary Theory Authors for 2006

D.P. Brennan, and L.E. Sugiyama "Tearing Mode Stability in a Low Beta Plasma with Sawteeth," Phys. Plasmas **13**, 052515 (2006).

D.P. Brennan, S.E. Kruger, D.D. Schnack, C.R. Sovinec, and A. Pankin "Computing Nonlinear Magnetohydrodynamic Edge Localized Instabilities in Fusion Plasmas," J. Phys.: Conf. Ser. **46**, 63 (2006).

J. Candy and R.E. Waltz, "Coupled ITG/TEM-ETG Gyrokinetic Simulation." Proc. 21st IAEA Fusion Energy Conf., Chengdu, China, 2006, Paper TH/2-1.

J. Candy, and R.E. Waltz "Velocity-Space Resolution, Entropy Production, and Upwind Dissipation in Eulerian Gyro-Kinetic Simulations," Phys. Plasmas **13**, 03231 (2006).

J. Candy, R.E. Waltz, S.E. Parker, and Y. Chen "Relevance of the Parallel Nonlinearity in Gyrokinetic Simulations of Tokamak Plasmas," Phys. Plasmas **13**, 074501 (2006).

V.S. Chan, A.D. Turnbull, M. Choi, M.S. Chu, L.L. Lao, "Monte-Carlo Simulation of High Harmonic Fast Wave Heating of Neutral Beam Ions and Effects on MHD Stability: Validation with Experiments," 2006 Varenna Theory of Fusion Plasmas Conference, AIP Conf. Proc. **871**, 27 (2006).

M. Choi, V.S. Chan, R.I. Pinsker, C.C. Petty, S.C. Chiu, J. Wright, P. Bonoli and M. Porkolab, "Simulation of Fast Alfvén Wave Interaction with Beam Ions over a Range of Cyclotron Harmonics in DIII-D Tokamak," Nucl. Fusion **46**, S409 (2006).

M.S. Chu, V.S. Chan, P.A. Politzer, D.P. Brennan, M. Choi, L.L. Lao, H.E. St. John, and A.D. Turnbull, "Kinetic Alfven Wave and Associated Current Drive at the Center of Tokamaks," Phys. Plasmas **13**, 114501 (2006).

C. Estrada-Mila, J. Candy, and R.E. Waltz "Density peaking and Turbulent Pinch in DIII-D Discharges," Phys. Plasmas **13**, 074505 (2006).

C. Estrada-Mila, J. Candy, and R.E. Waltz "Turbulent Transport of Alpha Particles and Helium Ash in Reactor Plasmas," Phys. Plasmas **13**, 112303 (2006).

F.L. Hinton and R.E. Waltz, "Gyrokinetic Turbulent Heating," Phys. Plasmas **13**, 102301 (2006).

J.E. Kinsey, R.E. Waltz, J. Candy "The Effects of Safety Factor and Magnetic Shear on Turbulent Transport in Nonlinear Gyro-Kinetic Simulations," Phys. Plasmas **13**, 022305 (2006).

P.B. Parks and F.W. Perkins, "A Gyrotron-Powered Pellet Accelerator for Tokamak Refueling," Nucl. Fusion **46**, 770 (2006).

G.M. Staebler, J.E. Kinsey and R.E. Waltz, "A Comprehensive Theory Based Transport Model," Proc. 21st IAEA Fusion Energy Conf., Chengdu, China, 2006, Paper TH/1-2.

G.M. Staebler and H.E. St. John "Predicted Toroidal Rotation Enhancement of Fusion Power Production in ITER," Nucl. Fusion **46**, L6 (2006).

R.E. Waltz, M.E. Austin, K.H. Burrell, and J. Candy, "Gyro-Kinetic Simulations of Off-Axis Minimum-q Profile Corrugations," Phys. Plasmas **13**, 052301 (2006).

R.E. Waltz, J. Candy, and C.C. Petty, "Projected Profile Similarity in Bohm and Gyro-Bohm Scaled DIII-D L- and H-Modes," Phys. Plasmas **13**, 072304 (2006)

7.3. Primary Theory Authors for 2005

D.P. Brennan, S.E. Kruger, T.A. Gianakon, D. Schnack "A Categorization of Tearing Mode Onset in Tokamaks via Nonlinear Simulation," Nucl. Fusion **45**, 1178 (2005).

J. Candy, "Beta Scaling of Transport in Microturbulence Simulations," Phys. Plasmas **12**, 072307 (2005).

M. Choi, V.S. Chan, R.I. Pinsker, S.C. Chiu, W.W. Heidbrink "Monte-Carlo Orbit/Full Wave Simulation of Ion Cyclotron Resonance Frequency Wave Damping on Resonant Ions in Tokamaks" Phys. Plasmas **12**, 072505 (2005).

M.S. Chu, M.S., K. Ichiguchi "Effect of the Resistive Wall on the Growth Rate of Weakly Unstable External Kink Mode in General 3D Configurations," Nucl. Fusion **45**, 804 (2005).

C. Estrada-Mila, J. Candy, R.E. Waltz, "Gyrokinetic Simulations of Ion and Impurity Transport," Phys. Plasmas **12**, 022305 (2005).

J.E. Kinsey, R.E. Waltz, J. Candy "Nonlinear Gyro-kinetic Simulations of E×B Shear Quenching of Transport," Phys. Plasmas **12**, 062302 (2005).

J.E. Kinsey, F. Imbeau, G. Staebler, et al., "Transport Modeling and Gyrokinetic Analysis of Advanced High Performance Discharges," Nucl. Fusion **45**, 450 (2005).

J.E. Kinsey, G.M. Staebler, R.E. Waltz "Predicting Core and Edge Transport Barriers in Tokamaks Using the GLF23 Drift Wave Transport Model," Phys. Plasmas **12**, 052503 (2005).

J.E. Kinsey, "GLF23 Modeling of Turbulent Transport in DIII-D," Fusion Sci. Tech. **48**, 1060 (2005).

L.L. Lao, H.E. St. John, Q. Peng, J.R. Ferron, E.J. Strait, T.S. Taylor "MHD Reconstruction in the DIII-D Tokamak," Fusion Sci. Tech. **48**, 968 (2005).

P.B. Parks, "A Model of Cusp Magnetic-Field Compression by an Expanding Plasma Fireball," Phys. Plasmas **12**, 102510 (2005).

P.B. Parks and L.R. Baylor, "Effect of Parallel Flows and Toroidicity on Cross-Field Transport of Pellet Ablation Matter in Tokamak Plasmas," Phys. Rev. Lett. **94**, 125002 (2005).

P.B. Snyder, H.R. Wilson, and X.Q. Xu, "Nonlinear Dynamics of ELMs: Numerical Studies of Flow Shear Effects and 3D Nonlinear ELM Dynamics" Phys. Plasmas **12**, 056115 (2005).

G.M. Staebler, J.E. Kinsey, and R.E. Waltz, "Gyro-Landau Fluid Equations for Trapped and Passing Particles," Phys. Plasmas **12**, 102508 (2005).

W.M. Tang and V.S. Chan "Advances and Challenges in Computational Plasma Science," Plasma Phys. Control. Fusion **47**, R1 (2005).

A.D. Turnbull, D.P. Brennan, M.S. Chu, L.L. Lao, P.B. Snyder, "Theory and Simulation Basis for Magnetohydrodynamic Stability in DIII-D," Fusion Sci. Tech. **48**, 875 (2005).

R.E. Waltz, J. Candy, F.L. Hinton, C. Estrada-Mila, J.E. Kinsey, "Advances in Comprehensive Gyro-kinetic Simulations of Transport in Tokamaks," Nucl. Fusion **45**, 741 (2005).

R.E. Waltz and J. Candy, "Heuristic Theory of Nonlocally Broken GyroBohm Scaling," Phys. Plasmas **12**, 072303 (2005).

R.E. Waltz, "ρ* Scaling of Physically Realistic Gyrokinetic Simulations of Transport in DIII-D," Fusion Sci. Tech. **48**, 1051 (2005).

S.K. Wong and V.S. Chan, "The Neoclassical Angular Momentum Flux in the Large Aspect Ratio Limit," Phys. Plasmas **12**, 092513 (2005).